Chart I

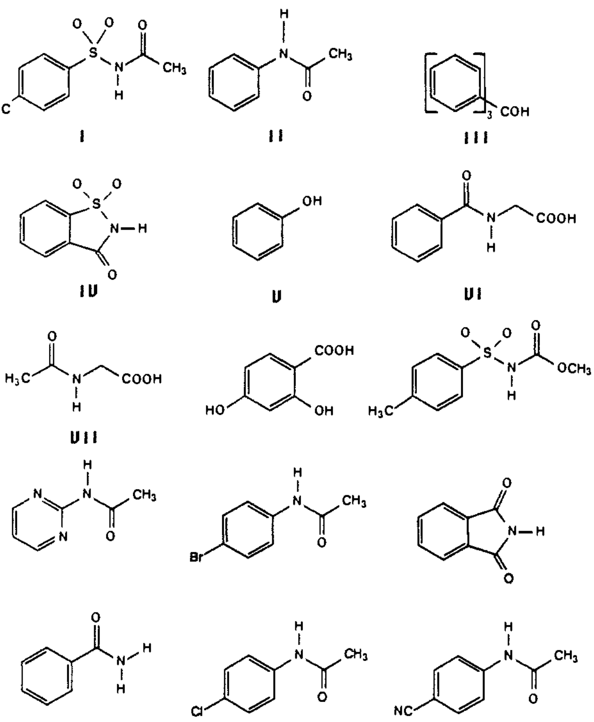

For I–V, crystals of the TPPO complex readily grew bigger and were of much higher quality than crystals of the substrate alone. For most of the other compounds in Chart I, crystals of the complex from toluene are chunky, while crystals of the substrates are thin needles or plates. We have not tried to optimize the size of any of these crystals. Triphenylcarbinol·TPPO gave the largest crystal, 0.1 × 1 × 2 cm. When substrates are not soluble in toluene, TPPO complexes can usually be formed from other solvents. For example, VI and VII were complexed with TPPO from a mixture of THF and H_2O. We were unable to obtain crystalline TPPO complexes of several compounds related to those in Chart I. Work is in progress to prepare these complexes.

There are two factors contributing to the effect that TPPO has on crystal growth properties. One involves the presence of a very strong hydrogen bond, necessary for complex formation, that imparts partial ionic character to the crystal. The other is the bulky shape of TPPO molecules which inhibits the formation of lamellar structures that cause crystals to fracture easily and to grow as thin plates. We are presently testing the importance of these two factors by studying the crystal habits of other hydrogen-bonded complexes.

Acknowledgment. We gratefully acknowledge Prof. Doyle Britton, University of Minnesota, for solving the crystal structure of I and ONR for partial support of this work. Helpful discussions with Tom Panunto, University of Minnesota, are also appreciated.

Registry No. I, 1888-33-1; II, 103-84-4; III, 76-84-6; IV, 81-07-2; V, 108-95-2; VI, 495-69-2; VII, 543-24-8; TPPO, 791-28-6; 2,4-dihydroxybenzoic acid, 89-86-1; methyl [(4-methylphenyl)sulfonyl]carbamate, 14437-03-7; *N*-2-pyrimidinylacetamide, 13053-88-8; *N*-(4-bromophenyl)acetamide, 103-88-8; 1*H*-isoindole-1,3(2*H*)-dione, 85-41-6; benzamide, 55-21-0; *N*-(4-chlorophenyl)acetamide, 539-03-7; *N*-(4-cyanophenyl)acetamide, 35704-19-9.

---

(16) Crystal data for I·TPPO: $C_{27}H_{26}NO_4PS$, $f_w = 491.6$, $a = 19.573$ (7) Å, $b = 13.470$ (14) Å, $c = 10.030$ (5) Å, $V = 2605.7$ Å^3, $P2_1/a$, $Z = 4$, $D_x = 1.25$ g/cc, Mo Kα, $R_w = 0.058$, $R = 0.048$ for 4362 reflections, $I > 1\sigma(I)$; Enraf-Nonius diffractometer, direct methods, full-matrix least-squares refinement, anisotropic temperature factors for non-hydrogen atoms, and isotropic temperature factors for hydrogen atoms, all of which were found on electron density difference maps. The –NH···O distance in the hydrogen bond is 2.705 (2) Å, and the N–H···O angle is 169.4 (2)°. Complete crystal structure details will be reported elsewhere.

Spectroscopic Evidence for the Formation of Singlet Molecular Oxygen ($^1\Delta_gO_2$) upon Irradiation of a Solvent-Oxygen ($^3\Sigma_g^-O_2$) Cooperative Absorption Band

Rodger D. Scurlock and Peter R. Ogilby*

Department of Chemistry, University of New Mexico
Albuquerque, New Mexico 87131

Received September 14, 1987

It is well-known that the presence of molecular oxygen ($^3\Sigma_g^-O_2$) in a variety of organic solvents causes an often substantial red shift in the solvent absorption spectrum.[1] This extra, broad absorption feature is reversibly removed by purging the solvent with nitrogen gas. Mulliken and Tsubomura assigned the oxygen-dependent absorption band to a transition from a ground state solvent–oxygen contact complex to a solvent–oxygen charge transfer (CT) state ($sol^{\bullet+}O_2^{\bullet-}$).[1] In addition to the broad Mulliken CT band, there are, often in the same spectral region, distinct singlet–triplet transitions ($T_1 \leftarrow S_0$) which are enhanced by molecular oxygen ($^3\Sigma_g^-O_2$).[2] Since both of these solvent–oxygen cooperative transitions may result in the formation of reactive oxygenating species, singlet molecular oxygen ($^1\Delta_gO_2$) and/or the superoxide ion ($O_2^{\bullet-}$), it follows that recent studies have focussed on unsaturated hydrocarbon oxygenation subsequent to the irradiation of the oxygen-induced absorption bands in both the solution phase and cryogenic (10 K) glasses.[3,4] In these particular experiments, oxygenated products characteristic of both $^1\Delta_gO_2$ and $O_2^{\bullet-}$ were obtained, although the systems studied appeared to involve the participation of one intermediate at the exclusion of the other.

In this communication, we provide, for the first time, direct spectroscopic evidence for the formation of $^1\Delta_gO_2$ following a solvent–oxygen ($^3\Sigma_g^-O_2$) cooperative absorption. We have observed, in a time-resolved experiment, a near-IR luminescence subsequent to laser excitation of the oxygen-induced absorption bands of mesitylene, *p*-xylene, *o*-xylene, toluene, and benzene at 355 nm and 1,4-dioxane at 266 nm. We suggest that this signal is due to $^1\Delta_gO_2$ phosphorescence.[5]

The following points are presented to support our claim that $^1\Delta_gO_2$ is indeed produced subsequent to irradiation of a solvent–oxygen absorption band.

1. The observed signal is $^1\Delta_gO_2$ phosphorescence. The λ_{max} of luminescence is 1270 nm, in agreement with previous $^1\Delta_gO_2$ assignments.[10-12] The lifetime of the time-resolved signal in each solvent, extrapolated to zero laser power, agrees with known $^1\Delta_gO_2$ lifetimes independently determined.[13,14] The addition of a $^1\Delta_gO_2$ quencher (sodium azide) to dioxane quenches the observed IR signal with a rate constant comparable to that known for $^1\Delta_gO_2$

---

* Author to whom correspondence should be addressed.

(1) Tsubomura, H.; Mulliken, R. S. *J. Am. Chem. Soc.* **1960**, *82*, 5966–5974.

(2) (a) Evans, D. F. *Nature* (*London*) **1956**, *178*, 534–353. (b) Evans, D. F. *J. Chem. Soc.* **1957**, 1351–1357.

(3) Onodera, K.; Furusawa, G.; Kojima, M.; Tsuchiya, M.; Aihara, S.; Akaba, R.; Sakuragi, H.; Tokumaru, K. *Tetrahedron* **1985**, *41*, 2215–2220.

(4) Hashimoto, S.; Akimoto, H. *J. Phys. Chem.* **1986**, *90*, 529–532.

(5) A complete description of the apparatus used to detect $^1\Delta_gO_2$ phosphorescence is reported elsewhere (ref 6–9). 355 nm and 266 nm correspond to the third and fourth harmonics, respectively, of a Nd:YAG pulsed laser. All $^1\Delta_gO_2$ phosphorescence experiments were performed in 1-cm cuvettes.

(6) Iu, K.-K.; Scurlock, R. D.; Ogilby, P. R. *J. Photochem.*, submitted for publication.

(7) Iu, K.-K.; Ogilby, P. R. *J. Phys. Chem.* **1987**, *91*, 1611–1617.

(8) Iu, K.-K.; Scurlock, R. D.; Ogilby, P. R. *J. Photochem.* **1987**, *37*, 19–32.

(9) Scurlock, R. D.; Ogilby, P. R. *J. Phys. Chem.* **1987**, *91*, 4599–4602.

(10) Khan, A. U. In *Singlet Oxygen, Volume I, Physical-Chemical Aspects*; Frimer, A. A., Ed.; CRC Press: Boca Raton, 1985; pp 39–79 and references cited therein.

(11) Ogilby, P. R.; Foote, C. S. *J. Am. Chem. Soc.* **1983**, *105*, 3423–3430.

(12) Hurst, J. R.: Schuster, G. B. *J. Am. Chem. Soc.* **1983**, *105*, 5756–5760.

(13) Monroe, B. M., in ref 10, pp 177–224 and references cited therein.

(14) τ(mesitylene) = 19 μs, τ(*p*-xylene) = 24 μs, τ(*o*-xylene) = 26 μs. τ(toluene) = 28 μs. τ(benzene) = 30 μs, τ(dioxane) = 26 μs.

0002-7863/88/1510-0640$01.50/0

quenching ($k_q \sim 5 \times 10^8$ s^{-1} M^{-1}).[15,16]

2. Neither a direct excitation of molecular oxygen (${}^3\Sigma_g^-O_2$) nor a $(O_2)_2$ simultaneous transition is responsible for the ${}^1\Delta_gO_2$ signal under our conditions.[10,17-20] Both cyclohexane and methanol can dissolve substantial amounts of oxygen[21] and exhibit oxygen-dependent absorption bands to the blue (<260 nm) of our pump wavelengths, but neither yield a ${}^1\Delta_gO_2$ signal when irradiated at 355 or 266 nm. It is expected that discrete oxygen transitions should be solvent independent. Furthermore, a plot of ${}^1\Delta_gO_2$ signal intensity (I_Δ) versus oxygen (${}^3\Sigma_g^-O_2$) concentration shows no positive curvature for any of the solvents mentioned above. This eliminates the possibility of a $(O_2)_2$ simultaneous absorption.

3. The I_Δ is linearly dependent on the excitation laser energy. This precludes a multiphoton absorption in the solvent and the subsequent formation of ${}^1\Delta_gO_2$ in a trivial sensitized process.

4. The excitation wavelengths used in our experiments are to the red of the solvent $S_1 \leftarrow S_0$ transition. Therefore, in a single photon absorption, the singlet excited electronic states of the solvent are energetically inaccessible.

5. The ${}^1\Delta_gO_2$ is not produced by an adventitious sensitizer either present as an impurity in the solvent or one which is photolytically created. Upon prolonged irradiation, I_Δ is constant, and the absorption spectra of the irradiated samples show no evidence of degradation. For each solvent, we are able to observe a small absorbance under nitrogen-purged conditions at the excitation wavelength using a 10 cm path length cell. In the case of mesitylene, *p*-xylene, *o*-xylene, and 1,4-dioxane, this absorbance can be reduced by successive distillation, indicating the presence of impurities in our samples. However, the reduction in the absorbance upon distillation is not accompanied by an equal reduction in I_Δ. To further show that these impurities are not responsible for ${}^1\Delta_gO_2$ formation, we prepared standard benzene solutions of a known ${}^1\Delta_gO_2$ sensitizer, acridine, such that the solution optical density (OD) at 355 nm was comparable to that of the impurity as measured in a nitrogen purged solvent. Acridine in benzene is an efficient ${}^1\Delta_gO_2$ sensitizer (quantum yield = 0.8).[6] The I_Δ obtained by pumping the oxygen (${}^3\Sigma_g^-O_2$) induced absorption bands in the aromatic solvents is at least three times greater than that observed for the standard acridine photosensitized ${}^1\Delta_gO_2$ signal. Although ${}^1\Delta_gO_2$ quantum yields of 2.0 are known, this phenomenon occurs at the limit of infinite oxygen concentration where all sensitizer singlet states are being quenched by ${}^3\Sigma_g^-O_2$.[6,22] At the oxygen concentrations used in our experiments, the results presented above indicate that if the impurity is indeed responsible for ${}^1\Delta_gO_2$ formation, it must have a ${}^1\Delta_gO_2$ quantum yield which far exceeds that of a standard photosensitized process.[6] Therefore, we conclude that ${}^1\Delta_gO_2$ is not produced by an adventitious sensitizer.

We suggest the observed ${}^1\Delta_gO_2$ will be formed primarily by a combination of two different channels: (1) a spin allowed, solvent–oxygen (${}^3\Sigma_g^-O_2$) cooperative transition to a triplet charge transfer state[1] with subsequent intersystem crossing and dissociation to yield ${}^1\Delta_gO_2$ and the ground state solvent molecule and (2) an oxygen (${}^3\Sigma_g^-O_2$) enhanced $T_1 \leftarrow S_0$ transition[2] followed by the sensitized formation of ${}^1\Delta_gO_2$ by the resulting triplet state. The wavelengths that correspond to the $T_1 \leftarrow S_0$ (0,0) absorption are as follows: benzene (340 nm),[2,23] toluene (346 nm),[24] *o*-xylene (348 nm),[24] *p*-xylene (355 nm),[24] and mesitylene (357 nm).[24] These distinct transitions are all found in the same spectral region as the broad, structureless Mulliken CT band. For benzene, toluene, and *o*-xylene, the excitation wavelength (355 nm)[5] is too far to the red to excite the $T_1 \leftarrow S_0$ transition. If the enhanced $T_1 \leftarrow S_0$ transition were the only channel responsible for the formation of the observed ${}^1\Delta_gO_2$, we would expect to see the ${}^1\Delta_gO_2$ signal only when *p*-xylene and mesitylene are pumped, and that the signal from *p*-xylene might be more intense than that from mesitylene. This is not the case. Rather, the I_Δ is linearly dependent on the OD of the oxygen-induced absorption at 355 nm for oxygenated benzene, toluene, *o*-xylene, and mesitylene. The *p*-xylene point, for which the $T_1 \leftarrow S_0$ transition is coincident with the excitation wavelength (355 nm), falls above the line, but I_Δ is not as large as that for mesitylene. Therefore, although some of the ${}^1\Delta_gO_2$ produced may be attributed to an oxygen-induced $T_1 \leftarrow S_0$ transition, we suggest that ${}^1\Delta_gO_2$ is also produced upon dissociation of a photolytically generated CT state.

In conclusion, we have provided direct spectroscopic evidence for the formation of ${}^1\Delta_gO_2$ subsequent to UV irradiation of a solvent–oxygen cooperative absorption band.

Acknowledgment. We thank Maria P. Dillon and Kai-Kong Iu for their assistance at various stages of this project. This work was supported by the National Science Foundation under Grant Number CHE-8501542.

---

(15) Wilkinson, F.; Brummer, J. G. *J. Phys. Chem. Ref. Data* **1981**, *10*, 809-999.

(16) A small amount of water was added to the solution in order to dissolve NaN$_3$.

(17) Rosenthal, I., in ref 10, pp 13-38 and references cited therein.

(18) (a) Eisenberg, W. C.; Taylor, K.; Veltman, J.; Murray, R. W. *J. Am. Chem. Soc.* **1982**, *104*, 1104-1105. (b) Eisenberg, W. C.; Snelson, A.; Butler, R.; Taylor, K.; Murray, R. W. *J. Photochem.* **1984**, *25*, 439-448.

(19) Koroll, G. W.; Singh, A. *Photochem. Photobiol.* **1978**, *28*, 611-613.

(20) Frei, H.; Pimentel, G. C. *J. Chem. Phys.* **1983**, *79*, 3307-3319.

(21) Battino, R., Ed. *IUPAC Solubility Data Series, Volume 7. Oxygen and Ozone*: Pergamon: Oxford, 1981; p 301.

(22) Dobrowolski, D. C.; Ogilby, P. R.; Foote, C. S. *J. Phys. Chem.* **1983**, *87*, 2261-2263.

(23) Sponer, H.; Kanda, Y.; Blackwell, L. A. *Spectrochim. Acta* **1960**, *16*, 1135-1147.

(24) Kanda, Y.; Shimada, R. *Spectrochim. Acta* **1961**, *17*, 279-285.

Use of $Ir_4(CO)_{11}$ To Measure the Lengths of Organic Molecules with a Scanning Transmission Electron Microscope

Frederic R. Furuya, Larry L. Miller,* J. F. Hainfeld,
William C. Christopfel, and Peter W. Kenny

Department of Chemistry, University of Minnesota
Minneapolis, Minnesota 55455
Biology Department, Brookhaven National
Laboratory, Upton, New York 11973

Received September 21, 1987

We report an evaluation of the hypothesis that metal-cluster labels can be used to accurately measure molecular distances by transmission electron microscopy (TEM). Organic and most small biological molecules are essentially transparent in TEM, but distances between molecular sites can in principle be measured by attachment of electron-dense clusters to those sites. The present test utilized a sufficiently long and rigid organic spacer with specifically attached $Ir_4(CO)_{11}$ labels and took advantage of the capabilities of scanning transmission electron microscopy (STEM) for high resolution measurements on molecular materials. $Ir_4(CO)_{11}$-labeled molecules, which have not previously been used for TEM, are shown to be synthetically accessible, sufficiently stable, and immobile in the electron beam so that they may have wider TEM applicability.

Electron microscopists have had a long standing interest in labeling molecular structures with metals. In order to take advantage of the high resolution of modern microscopes and achieve specificity in imaging, attention has been given to metal clusters. Two types of clusters have been studied: anionic heteropolytungstates,[1,2] e.g., $(RC_5H_4)TiP_2W_{17}O_{61}{}^{7-}$, and cationic undecagold clusters,[3] e.g., $Au_{11}(CN)_3[P(C_6H_4CH_2NH_3{}^+)_3]_7$. Molecular

---

* Address correspondence to author at University of Minnesota.

(1) (a) Keana, J. F. W.; Ogan, M. D.; Lu, Y.; Beer, M.; Varkey, J. *J. Am. Chem. Soc.* **1985**, *107*, 6714. (b) Keana, J. F. W.; Ogan, M. D. *J. Am. Chem. Soc.* **1986**, *108*, 7951. (c) Keana, J. F. W.; Ogan, M. D.; Lu, Y.; Beer, M.; Varkey, J. *J. Am. Chem. Soc.* **1986**, *108*, 7956.

(2) Monson, K. L.; Wall, J. S.; Hainfeld, J. F. *Ultramicroscopy* **1987**, *21*, 147.

(3) (a) Safer, D.; Hainfeld, J. F.; Wall, J. S.; Riordan, J. *Science (Washington, D. C.)* **1982**, *218*, 290. (b) Frey, P. A.; et al. *Biochemistry* **1984**, *23*, 3849, 3857, 3863. (c) Safer, D.; Bolinger, L.; Leigh, J. S. *J. Inorg. Biochem.* **1986**, *26*, 77. (d) Lipka, J. J.; Hainfeld, J. F.; Wall, J. S. *J. Ultrastruct. Res.* **1983**, *84*, 120.

0002-7863/88/1510-0641$01.50/0